

## How Antiferromagnetism Drives the Magnetization of a Ferromagnetic Thin Film to Align Out of Plane

Bo-Yao Wang,<sup>1</sup> Jhen-Yong Hong,<sup>1</sup> Kui-Hon Ou Yang,<sup>1</sup> Yuet-Loy Chan,<sup>2</sup>  
Der-Hsin Wei,<sup>2</sup> Hong-Ji Lin,<sup>2</sup> and Minn-Tsong Lin<sup>1,3,\*</sup>

<sup>1</sup>*Department of Physics, National Taiwan University, Taipei 10617, Taiwan*

<sup>2</sup>*National Synchrotron Radiation Research Center, Hsinchu 300, Taiwan*

<sup>3</sup>*Institute of Atomic and Molecular Sciences, Academia Sinica, Taipei 10617, Taiwan*

(Received 30 September 2012; revised manuscript received 7 January 2013; published 12 March 2013)

Interfacial moments of an antiferromagnet are known for their prominent effects of induced coercivity enhancement and exchange bias in ferromagnetic-antiferromagnetic exchange-coupled systems. Here we report that the unpinned moments of an antiferromagnetic face-centered-cubic Mn layer can drive the magnetization of an adjacent Fe film perpendicular owing to a formation of intrinsic perpendicular anisotropy. X-ray magnetic circular dichroism and hysteresis loops show establishment of perpendicular magnetization on Fe/Mn bilayers while temperature was decreased. The fact that the magnitude of perpendicular anisotropy of the Fe layer is enhanced proportionally to the out-of-plane oriented orbital moment of the Mn unpinned layer, rather than that of Fe itself, gives evidence for the Mn unpinned moments to be the origin of the established perpendicular magnetization.

DOI: [10.1103/PhysRevLett.110.117203](https://doi.org/10.1103/PhysRevLett.110.117203)

PACS numbers: 75.50.Ee, 75.30.Gw, 75.70.-i

Antiferromagnets, a class of magnetic materials with rich physics and potential application had been underestimated for a long time in history because of lack of macroscopic magnetization and insensitivity to the external magnetic field. The revival has been made upon placing it next to a ferromagnet [1–4], where the effects of induced coercivity ( $H_c$ ) enhancement and exchange bias can be applied to the design of magnetic logic devices like the spin valve, for “pinning” the magnetization of a magnetic reference layer under magnetization switching of a magnetic storage layer [5]. Based on research efforts in the last few years [6–12],  $H_c$  enhancement and exchange bias have been understood to be correlated with the so-called “unpinned” and uncompensated “pinned” moments of an antiferromagnet close to the interface, respectively.

However, recent discoveries make the antiferromagnet even more fascinating. It has been found that a single crystalline antiferromagnetic (AFM) fcc Mn ultrathin film can change the magnetization of adjacent ferromagnetic (FM) layers from the in-plane to the out-of-plane direction [13]. This finding could be extended, by choosing suitable FM layer and tuning the thickness of both FM and AFM layers, to the application of a precise control of perpendicular anisotropy of magnetic storage layers within the soft magnetic regime [14], and therefore benefits the design of perpendicular-based spintronic device utilizing state-of-the-art spin-transfer torque [15–17]. More importantly, this finding shows essential aspects of magnetism of antiferromagnets that have not been explored.

In this Letter, by monitoring the magnetic moments with element resolution, we perform experimental evidence to unveil the AFM nature that induces the perpendicular magnetization of an adjacent FM layer. We show a

formation of perpendicular anisotropy through the unpinned moments of the Mn layer at the interface, which drives the magnetization of the adjacent Fe layer from the in-plane to the perpendicular direction. This finding provides renewed functionality for the interfacial moments of the AFM layer that has for a long time primarily been known to be responsible for  $H_c$  enhancement and exchange bias phenomena.

The magnetic ultrathin films were prepared in a UHV NTU-NSRRC nanomagnetism preparation chamber with a base pressure of  $2 \times 10^{-10}$  Torr. The  $\text{Cu}_3\text{Au}(001)$  single crystal with  $0.1^\circ$  miscut was used as the substrate, in which the preparation procedure is described in previous reports [13,18]. The ultrathin Fe/Mn films were deposited on  $\text{Cu}_3\text{Au}(001)$  at room temperature, and the growth rates were monitored by medium energy electron diffraction [18,19]. The structure of the films was characterized by low energy electron diffraction (LEED) and LEED  $I$ - $V$  measurements. The result suggests that significant structural effects on the magnetic properties of Fe/Mn bilayers can be excluded [13].

Element-resolved magnetic domain images (Fe and Mn) of bilayers were measured *in situ* by photoemission electron microscopy (PEEM) utilizing x-ray magnetic circular dichroism (XMCD) effect at beam line BL05B2 of NSRRC in Hsinchu, Taiwan. As described in previous studies [13,19], the magnetic information of individual elements can be obtained from the asymmetry of the XMCD curve at the  $L_{3,2}$  absorption edges. Combining XMCD and PEEM, the full-field view of the emitted secondary electrons from the magnetic sample can be resolved by a multichannel plate and recorded by a CCD camera. The contrast normalization is achieved by doing

imaging calculation on the two full-field images, taken at the Fe (or Mn)  $L_{3,2}$  and  $L_2$  edges, respectively [19]. In the present Letter, the magnetic imagings were performed in the as-grown condition and at 120 K. For measuring the XMCD curves and element-specific magnetic hysteresis loops, the samples were transferred to the XMCD measurement chamber at beam line BL11A1 of NSRRC under UHV conditions, by a small mobile UHV chamber. The XMCD curves for sum-rule analysis were derived from the  $L_{3,2}$ -edge x-ray absorption spectra measured at  $\pm 2600$  Oe with a fixed incident x-ray polarization  $\sim 78\%$  in total electron yield (TEY) mode. The element-resolved hysteresis loops were acquired by recording the magnetic asymmetry at  $L_{3,2}$  edges in x-ray absorption spectra with variation of magnetic field. The geometries for both XMCD curve and hysteresis loop measurements (at both in-plane and out-of-plane directions) are described by the illustrations of Fig. 1.

A brief introduction for the magnetic properties of Fe/Mn bilayers is presented first. Figure 1(a) shows the hysteresis loops of the 6 ML Fe/Mn bilayers contributed by the Fe layer. The magnetization of the Fe film aligns in the in-plane direction as the Mn film thickness ( $t_{\text{Mn}}$ ) at low coverage, and then changes to the out-of-plane direction as  $t_{\text{Mn}}$  is increased. This presents a phenomenon of in-plane to out-of-plane spin-reorientation transition (SRT) which is consistent with data reported previously [13]. The SRT can also be achieved by varying temperature. Figure 1(b) shows the  $H_c$  of 6 ML Fe/7, 10 ML Mn bilayers with temperature dependence. It is found that 6 ML Fe/7 ML Mn and 6 ML Fe/10 ML Mn bilayers exhibit temperature-dependent SRT from out-of-plane to in-plane direction as the temperature above  $T_{\text{SRT}}^a \sim 235$  K and  $T_{\text{SRT}}^b \sim 260$  K,

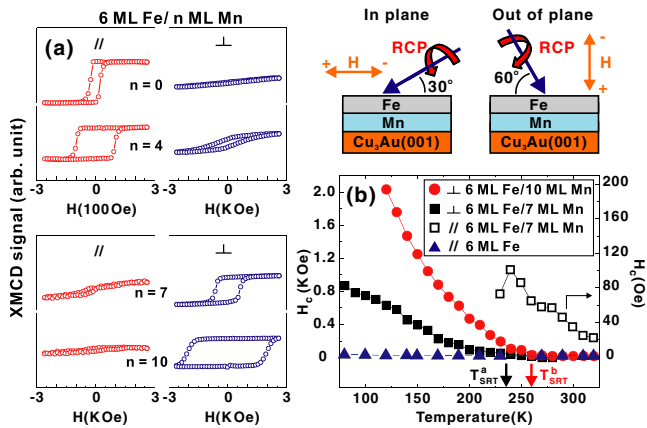


FIG. 1 (color online). (a) Magnetic hysteresis loops of the 6 ML Fe/ $n$  ML Mn bilayers measured by XMCD at the Fe  $L_{3,2}$  edges at 120 K. The illustrations indicate the in-plane and out-of-plane geometries for the XMCD measurements. (b) Temperature-dependent coercivity ( $H_c$ ) for the 6 ML Fe/0, 7, 10 ML Mn bilayers.  $T_{\text{SRT}}^a$  and  $T_{\text{SRT}}^b$  are the spin-reorientation transition temperatures of the 6 ML Fe/7 ML Mn and 6 ML Fe/10 ML Mn, respectively.

respectively. The enhanced thermal stability of the perpendicular magnetization (from  $T_{\text{SRT}}^a$  to  $T_{\text{SRT}}^b$ ) with an increase of  $t_{\text{Mn}}$  could originate from the finite-size effect of AFM ultrathin film [13,20]. A dramatically enhanced  $H_c$  for the perpendicular magnetic films at low temperature is in sharp contrast to the finding of only slightly enhanced  $H_c$  in in-plane magnetic Co-capped 6 ML Fe/7, 10 ML Mn bilayers [21]. This indicates a well-established out-of-plane-oriented exchange coupling between Fe and Mn layers.

The investigation of magnetic properties of the Mn layer was first performed by the magnetic domain imaging with XMCD-PEEM. For the 6 ML Fe/6 ML Mn bilayer as shown in Figs. 2(a) and 2(b), the Mn layer reveals net FM moments with its domain boundary the same as to the Fe layer. Since no FM characteristic was observed for the Mn layer alone, the presence of long range FM ordering on the Mn layer could be induced by a direct exchange coupling with the adjacent FM layer [7–12,22]. The finding of the opposite magnetic asymmetry between the Mn and Fe moments indicates a preference of antiparallel type exchange coupling [23]. To further clarify the characteristics of the present Mn moments and its correlation with the Fe moments, measurements of element-specific hysteresis loops with temperature dependence were performed. Figure 2(c) shows the selected Fe and Mn hysteresis loops of the 6 ML Fe/8 ML Mn bilayer measured for the out-of-plane direction. It is clear that not only the Fe but also the Mn shows the magnetic hysteresis loops. A finding of “inverse” hysteresis loops between the Fe and Mn moments confirms its preference of antiparallel type

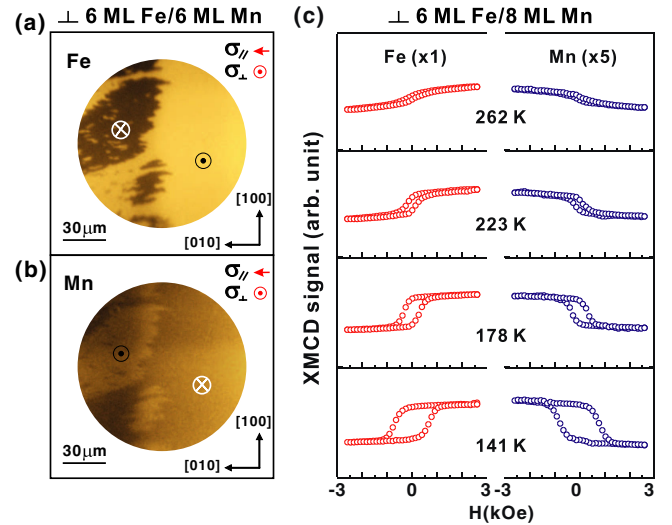


FIG. 2 (color online). (a) and (b) Magnetic domain images of the 6 ML Fe/6 ML Mn bilayer measured at the  $L_{3,2}$  edges of Fe and Mn elements at 120 K. (c) Temperature-dependent magnetic hysteresis loops of the 6 ML Fe/8 ML Mn bilayer measured by XMCD at the Fe and Mn  $L_{3,2}$  edges and at the out-of-plane direction. It is noted that a use of the 8 ML Mn film in temperature-dependent measurement is for gaining the higher thermal stability of perpendicular magnetization.

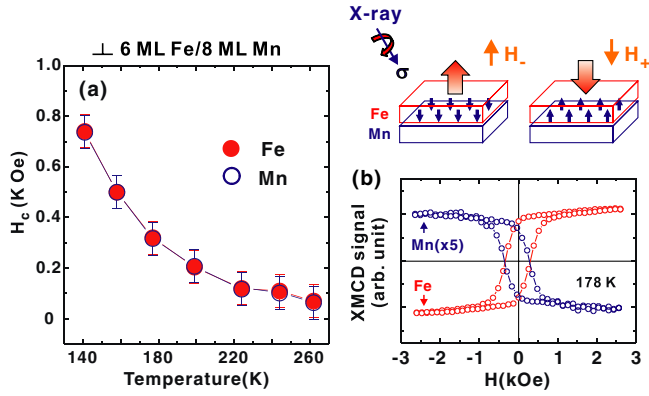


FIG. 3 (color online). (a) Coercivity  $H_c$  of the Fe and Mn magnetic hysteresis loops for the 6 ML Fe/8 ML Mn bilayer with temperature dependence measured for the out-of-plane direction. (b) The represented Fe and Mn hysteresis loops at 178 K, which show nearly the same  $H_c$  between the Fe and Mn moments. The illustrations describe the characteristic of the unpinned moments of Mn layer formed at Fe-Mn interface under external magnetic fields.

exchange coupling as obtained from magnetic imaging [Fig. 1]. Figure 3(a) shows the  $H_c$  of both elements for the 6 ML Fe/8 ML Mn bilayer as a function of temperature. As demonstrated by the selected hysteresis loops in Fig. 3(b), the Mn moments show nearly the same  $H_c$  with the Fe moments at various temperatures. This reveals itself

as the unpinned moments or rotatable moments of the AFM Mn layer close to the FM-AFM interface [7–9]. Inspired by the previous works demonstrating that the interfacial moments of AFM layer in a FM/AFM bilayer are crucial for the exchange bias or coercivity enhancement [7–9], the Mn unpinned moments in the present case are also expected to be associated with the phenomenon of an established perpendicular magnetization of the Fe film in the Fe/Mn bilayers.

According to prior works [27,28], the magnetic anisotropy of a low dimensional magnetic thin film is usually given by the crystalline anisotropy originating from the spacial anisotropy of the orbital moments. For a magnetic system with strong uniaxial crystalline anisotropy, the magnitude of crystalline anisotropy is linked with the ratio of orbital to spin moments in the magnetic easy direction [21]. This information can be obtained by analyzing the XMCD curves with the well-developed XMCD sum rules [29–31]. In the present case, the same approach is applied to probe the crystalline anisotropy of both Mn unpinned moments and Fe moments for a detailed understanding of the characteristic of Mn unpinned moments and clarifying the origin of an established perpendicular magnetization in the Fe/Mn bilayers.

Figures 4(a), 4(b), 4(d), and 4(e) show the represented Mn and Fe  $L_{3,2}$ -edge XMCD curves of the 6 ML Fe/8 ML Mn bilayer measured at different temperatures of 199 and

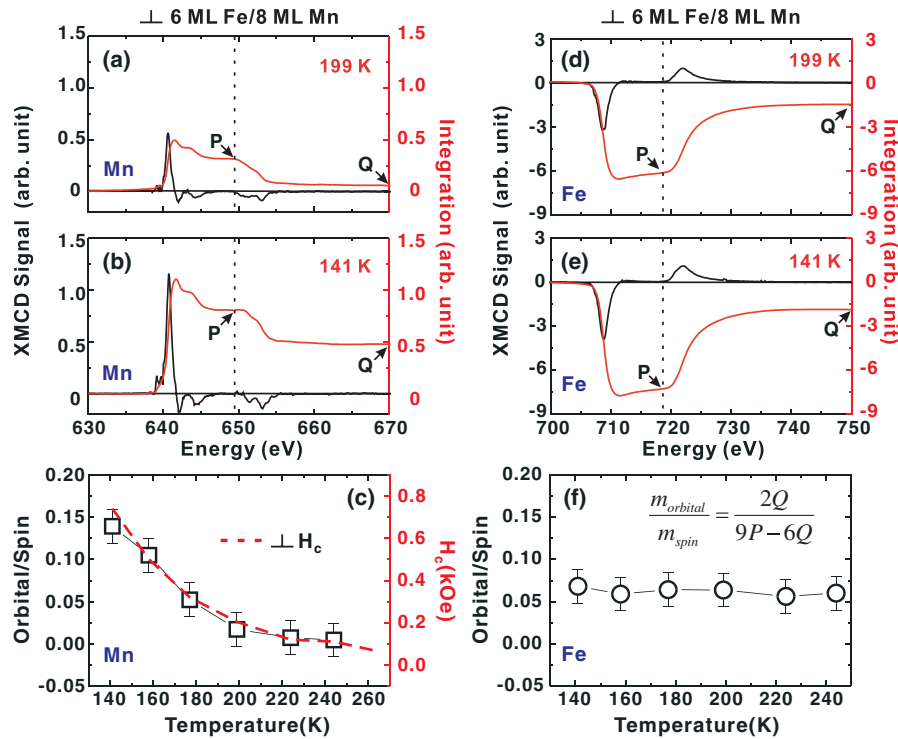


FIG. 4 (color online). Selected Mn [(a),(b)] and Fe [(d),(e)]  $L_{3,2}$ -edge XMCD curves of the 6 ML Fe/8 ML Mn bilayer measured at 199 and 141 K. The red or gray solid lines show the integrated curves, described by the right axis. (c) and (f) The  $m_{orbital}^{\perp}/m_{spin}^{\perp}$  ratio of Mn and Fe moments, respectively, calculated by  $P$  and  $Q$  values according to the formula shown in inset of (f) [29–31,33]. In (c), the red dashed line indicates the  $H_c$  of 6 ML Fe/8 ML Mn bilayer measured for the out-of-plane direction.

141 K, respectively. The  $P$  and  $Q$  values given by the integration of XMCD curves (red or gray solid lines) in  $L_3$  and  $L_3 + L_2$  regions indicate the sum of magnetic asymmetry in both regions, respectively. With the assumption of a negligible magnetic dipole operator term in the spin sum rule [29,30] which is small for  $3d$  metals [32],  $P$  and  $Q$  values can be used to calculate the ratio of orbital to spin moments according to the formula of  $m_{\text{orbital}}^{\perp}/m_{\text{spin}}^{\perp} = 2Q/(9P - 6Q)$  [31], and obtain the information of crystalline anisotropy. Since the XMCD curves in the present Letter were measured in the condition of flipping magnetization but fixed photohelicity of circular polarized x ray, in the case of Mn element, the calculated orbital to spin moments ratios are thus contributed only by unpinned moments of Mn layer. Figure 4(c) shows the orbital to spin ratio of the Mn unpinned moments at various temperatures [33]. The significant enhancement of the ratio with a decrease of temperature indicates an establishment of perpendicular crystalline anisotropy for the Mn unpinned moments [21]. Within the same temperature range, however, the ratio for the Fe moments in Fig. 4(f) remains a similar value. This indicates the perpendicular crystalline anisotropy of the Fe film is nearly invariant, and its major contribution to an established perpendicular magnetization can therefore be excluded. Thus, according to the finding of similar temperature-dependent tendency between the perpendicular  $H_c$  (red dashed line) and  $m_{\text{orbital}}^{\perp}/m_{\text{spin}}^{\perp}$  of the Mn [Fig. 4(c)] [21], an established perpendicular magnetization of the Fe layer could be induced by the Mn unpinned moments with a strongly enhanced perpendicular crystalline anisotropy at low temperature.

To further confirm the origin of an established perpendicular magnetization in Fe/Mn bilayer, the quantitative value of crystalline anisotropy energy ( $K_{\text{cry}}$ ) of the Mn unpinned moments was calculated according to the prior theoretical works [27,28]. As described in detail in the Supplemental Material [21], a  $K_{\text{cry}}$  of about  $3.85 \pm 0.50$  meV/atom was obtained for the 6 ML Fe/8 ML Mn bilayer at 141 K (assuming all the Mn unpinned moments at interface). The total perpendicular anisotropy energy of Mn unpinned moments that includes the shape anisotropy ( $-0.53$  meV/atom) was estimated to be  $3.32 \pm 0.50$  meV/atom. This energy value is found to be close to the enhanced anisotropy energy of the perpendicular magnetization of the Fe film (about  $3.02 \pm 0.65$  meV/atom) simulated via Néel type phenomenological magnetic anisotropy model in previous work [13,35]. This further gives evidence that the anisotropy of the Mn unpinned moment to be the origin of an established perpendicular magnetization of the Fe film in the Fe/Mn bilayers.

The presence of perpendicular crystalline anisotropy on the Mn unpinned moments is expected to originate from the AFM ordering of the fcc Mn layer. Even though a direct measurement on the AFM spin configuration of the fcc Mn layer has not been achieved so far, Hafner and Spišák

found spin spiral solutions at the  $X$  and  $L$  points for a free standing fcc Mn layer [36]. The latter solution, which corresponds to the [111]-layered AFM structure, confirms a possible existence of perpendicular crystalline anisotropy on the interfacial spin moments of the fcc Mn layer. Nevertheless, a [111] layered AFM structure may imply a compensated AFM spin order at [001] surface. Therefore, combining the present experimental finding of unpinned moments with perpendicular crystalline anisotropy and the theoretical result yields an interesting possibility that the interfacial Mn moments may keep their perpendicular crystalline anisotropy inherent from the bulk AFM ordering of the fcc Mn layer, even though a long range ferromagnetic ordering (i.e., unpinned moment) can be induced by the adjacent FM layer. This speculation is actually consistent with the finding on the interfacial unpinned moments of Co/FeF<sub>2</sub> bilayer reported previously [9].

On the other hand, although the established perpendicular magnetization of the Fe film is attributed to the unpinned moments of the Mn layer at Fe/Mn interface, according to our previous work [13], its magnitude can be supported by the underlying pinned moments of the Mn layer, following the finite-size tendency [20]. To our knowledge, these pinned moments can usually be classified into the “compensated” and “uncompensated” pinned moments. The “uncompensated” pinned moments are found to occur coincidentally with the established exchange bias in FM/AFM bilayer [7–9]. In the present case, since the exchange bias was not observed in most of the FM/Mn bilayers (i.e., Mn thickness  $< 12$  ML) even though the perpendicular magnetization is well established, the “uncompensated” pinned Mn moments are expected to be absent or very tiny in the most “thin” Mn layers [13,14]. On the other hand, although the remaining “compensated” pinned Mn moments cannot be directly sensed by the XMCD measurement due to the cancellation of net magnetization, the thermal stability of AFM ordering is expected to be enhanced while the thickness is increased, and the tendency can usually be described by the finite-size scaling phenomenological model [20]. Thus, once the AFM ordering of “compensated” pinned Mn moments becomes more “robust” because of increased thickness, a coupling could result in a raising of the thermal stability of the perpendicular crystalline anisotropy of the unpinned Mn moments, and lead to an enhancement of the magnitude of the perpendicular magnetization for the Fe layer.

In conclusion, we have reported a new feature of the AFM Mn layer with the unpinned moments that leads to establishment of perpendicular magnetization in the adjacent Fe layer. Our experimental result clearly indicates that the induced perpendicular magnetization of the Fe layer is directly correlated with the orbital moments of the Mn unpinned layer, rather than that of the Fe film itself. A combination of present and previous works [13,14] suggests an interesting picture that although the established

perpendicular magnetization of the Fe film is attributed to the unpinned moments of the Mn layer at Fe/Mn interface, the thermal stability is supported by the underlying “compensated” pinned moments of the Mn layer through the finite-size effect [20]. The effect demonstrated here shows an aspect other than the well-investigated phenomena of coercivity enhancement and exchange bias and renews our knowledge on the roles of the magnetic moments of the AFM layer in nanomagnetism. This will also open an avenue for fundamental understanding of antiferromagnetism in general and provide a firm basis for the future design of the perpendicular-based magnetic or spintronic nanodevices.

This work was supported in part by the National Science Council of Taiwan through Grants No. NSC 100-2120-M-002-002 and No. 101-2120-M-002-012.

\*To whom all correspondence should be addressed.

mtlin@phys.ntu.edu.tw

- [1] W. H. Meiklejohn and C. P. Bean, *Phys. Rev.* **102**, 1413 (1956).
- [2] W. H. Meiklejohn and C. P. Bean, *Phys. Rev.* **105**, 904 (1957).
- [3] J. Nogués and I. K. Schuller, *J. Magn. Magn. Mater.* **192**, 203 (1999).
- [4] S. D. Bader, *Rev. Mod. Phys.* **78**, 1 (2006).
- [5] S. Mao, Z. Gao, H. Xi, P. Kolbo, M. Plumer, L. Wang, A. Goyal, I. Jin, J. Chen, C. Hou, R. M. White, and E. Murdock, *IEEE Trans. Magn.* **38**, 26 (2002).
- [6] F. Nolting, A. Scholl, J. Stöhr, J. W. Seo, J. Fompeyrine, H. Siegart, J. P. Locquet, S. Anders, J. Luning, E. E. Fullerton, M. F. Toney, M. R. Scheinfein, and H. A. Padmore, *Nature (London)* **405**, 767 (2000).
- [7] S. Roy, M. R. Fitzsimmons, S. Park, M. Dorn, O. Petravic, I. V. Roshchin, Z. P. Li, X. Battle, R. Morales, A. Misra, X. Zhang, K. Chesnel, J. B. Kortright, S. K. Sinha, and I. K. Schuller, *Phys. Rev. Lett.* **95**, 047201 (2005).
- [8] H. Ohldag, A. Scholl, F. Nolting, E. Arenholz, S. Maat, A. T. Young, M. Carey, and J. Stöhr, *Phys. Rev. Lett.* **91**, 017203 (2003).
- [9] H. Ohldag, H. Shi, E. Arenholz, J. Stöhr, and D. Lederman, *Phys. Rev. Lett.* **96**, 027203 (2006).
- [10] J. S. Park, J. Wu, E. Arenholz, M. Liberati, A. Scholl, Y. Meng, C. Hwang, and Z. Q. Qiu, *Appl. Phys. Lett.* **97**, 042505 (2010).
- [11] Y. Meng, J. Li, A. Tan, E. Jin, J. Son, J. S. Park, A. Doran, A. T. Young, A. Scholl, E. Arenholz, J. Wu, C. Hwang, H. W. Zhao, and Z. Q. Qiu, *Appl. Phys. Lett.* **98**, 212508 (2011).
- [12] Y. Meng, J. Li, A. Tan, J. Park, E. Jin, H. Son, A. Doran, A. Scholl, E. Arenholz, H. W. Zhao, C. Hwang, and Z. Q. Qiu, *Phys. Rev. B* **84**, 064416 (2011).
- [13] B. Y. Wang, N. Y. Jih, W. C. Lin, C. H. Chuang, P. J. Hsu, C. W. Peng, Y. C. Yeh, Y. L. Chan, D. H. Wei, W. C. Chiang, and M. T. Lin, *Phys. Rev. B* **83**, 104417 (2011).
- [14] N. Y. Jih, B. Y. Wang, Y. L. Chan, D. H. Wei, and M. T. Lin, *Appl. Phys. Express* **5**, 063008 (2012).
- [15] S. Ikeda, K. Miura, H. Yamamoto, K. Mizunuma, H. D. Gan, M. Endo, S. Kanai, J. Hayakawa, F. Matsukura, and H. Ohno, *Nat. Mater.* **9**, 721 (2010).
- [16] D. C. Worledge, G. Hu, D. W. Abraham, J. Z. Sun, P. L. Trouilloud, J. Nowak, S. Brown, M. C. Gaidis, E. J. O’Sullivan, and R. P. Robertazzi, *Appl. Phys. Lett.* **98**, 022501 (2011).
- [17] K. Yakushiji, T. Saruya, H. Kubota, A. Fukushima, T. Nagahama, S. Yuasa, and K. Ando, *Appl. Phys. Lett.* **97**, 232508 (2010).
- [18] W. C. Lin, T. Y. Chen, L. C. Lin, B. Y. Wang, Y. W. Liao, K. J. Song, and M. T. Lin, *Phys. Rev. B* **75**, 054419 (2007).
- [19] B. Y. Wang, C. H. Chuang, S. S. Wong, J. J. Chiou, W. C. Lin, Y. L. Chan, D. H. Wei, and M. T. Lin, *Phys. Rev. B* **85**, 094412 (2012).
- [20] T. Ambrose and C. L. Chien, *Phys. Rev. Lett.* **76**, 1743 (1996).
- [21] See Supplemental Material at <http://link.aps.org/supplemental/10.1103/PhysRevLett.110.117203> for information of preferred orientation of Fe-Mn exchange coupling and correlation between crystalline anisotropy energy and orbital/spin ratio.
- [22] F. Offi, W. Kuch, L. I. Chelaru, K. Fukumoto, M. Kotsugi, and J. Kirschner, *Phys. Rev. B* **67**, 094419 (2003).
- [23] According to Refs. [24–26], the imaginary part of the charge and magnetic scattering factors for both metallic Fe and Mn unpinned moments have the same sign. The Fe moments and Mn unpinned moments are therefore confirmed to couple antiparallely.
- [24] A. Déchelette, J. M. Tonnerre, M. C. Saint Lager, F. Bartolomé, L. Sève, D. Raoux, H. Fischer, M. Piecuch, V. Chakarian, and C. C. Kao, *Phys. Rev. B* **60**, 6636 (1999).
- [25] S. Brück, S. Macke, E. Goering, X. Ji, Q. Zhan, and K. M. Krishnan, *Phys. Rev. B* **81**, 134414 (2010).
- [26] W. L. O’Brien and B. P. Tonner, *Phys. Rev. B* **50**, 2963 (1994).
- [27] J. Stöhr and H. C. Siegmann, *Magnetism: From Fundamentals to Nanoscale Dynamics* (Springer, New York, 2006), illustrated ed.
- [28] P. Bruno, *Phys. Rev. B* **39**, 865 (1989).
- [29] B. T. Thole, P. Carra, F. Sette, and G. van der Laan, *Phys. Rev. Lett.* **68**, 1943 (1992).
- [30] P. Carra, B. T. Thole, M. Altarelli, and X. Wang, *Phys. Rev. Lett.* **70**, 694 (1993).
- [31] C. T. Chen, Y. U. Idzerda, H. J. Lin, N. V. Smith, G. Meigs, E. Chaban, G. H. Ho, E. Pellegrin, and F. Sette, *Phys. Rev. Lett.* **75**, 152 (1995).
- [32] R. Wu, D. Wang, and A. J. Freeman, *Phys. Rev. Lett.* **71**, 3581 (1993).
- [33] A correction vector 1.5 was considered in spin sum rule of Mn unpinned moments due to suggested overlap between  $2P_{3/2}$  and  $2P_{1/2}$  states [34]. A near constant error of the orbital/spin ratio for the Mn unpinned moments could be attributed to a cancellation of the uncertainty caused by the number of holes, the angle between x-ray beam and sample, and the degree of circular polarization.
- [34] Y. Teramura, A. Tanaka, and T. Jo, *J. Phys. Soc. Jpn.* **65**, 1053 (1996).
- [35] L. Néel, C. R. Hebd. Seances Acad. Sci. **237**, 1468 (1953); *J. Phys. Radium* **15**, 225 (1954).
- [36] J. Hafner and D. Spišák, *Phys. Rev. B* **72**, 144420 (2005).